Contract No:

This document was prepared in conjunction with work accomplished under Contract No. DE-AC09-08SR22470 with the U.S. Department of Energy (DOE) Office of Environmental Management (EM).

Disclaimer:

Drift in Open-Circuit Potential of Carbon Steel in Nuclear Waste Simulants

Pavan K. Shukla, Roderick E. Fuentes, and Bruce J. Wiersma
Savannah River National Laboratory®
Aiken, South Carolina, 29808
USA

and

Crystal Girardot, Natalie Young, and Theodore Venetz
Washington River Protection Solutions
2425 Stevens Center Pl
Richland, Washington, 99352
USA

ABSTRACT

Millions of gallons of high-level radioactive waste are stored in underground carbon-steel storage tanks at the Hanford site. The waste chemistries are alkaline with pH between 11 and 14. Carbon steel is expected to become passive and undergo passive dissolution under the alkaline conditions. Nonetheless, certain corrosive species in the waste chemistries, such as chloride and nitrate, could cause pitting corrosion and stress corrosion cracking (SCC). The risk of pitting corrosion and SCC increases when open-circuit potentials (OCPs) drift in anodic direction compared to the initial values; it is important to determine the extent of drift as a function of waste chemistry and metal surface characteristics. Electrochemical experiments were conducted to determine extent of drift in the OCPs. The tests were conducted with the following three surface characteristics: (i) polished surface by sanding a coupon, (ii) surface with mill-scale plus corrosion product, and (iii) partially removed mill-scale plus corrosion products. Coupons were immersed in a waste simulant for several months and OCPs were recorded. Several other electrochemical techniques were used to measure corrosion-related properties. Experimental data demonstrated that terminal OCPs are independent of surface conditions.

Key words: Open-circuit potential, passive film, Hanford, high-level radioactive waste

INTRODUCTION

Approximately 55 million gallons of radioactive waste is being stored in 177 carbon steel tanks at Hanford. Long-term performance and integrity of the tanks is partly dependent on modifying the waste chemistry such that risk of pitting and stress corrosion cracking of the tank carbon-steel are mitigated. To this end, cyclic potentiodynamic polarization (CPP) experiments are conducted to identify risk of pitting corrosion, and subsequently determine the level of inhibition needed to mitigate the pitting corrosion. One of the key parameters associated with the determination is the difference between the corrosion and repassivation potentials: if the corrosion potential is greater than repassivation potential, the risk of pitting corrosion exists. Corrosion potential is defined as steady-state value of open circuit potential. CPP experiments are conducted as per a procedure derived from ASTM G61, and the current versus potential measurements are started two hours after an experiment has been setup.[1] The derived procedure is slightly different from the one detailed in ASTM G61.[2,3]

CPP experiment data is generally used to measure tendency of repassivation including repassivation potential, and it is assumed that corrosion potential is held steady during the measurement and thereafter. It is implicitly assumed that the corrosion potential measured at the start of CPP is sufficient for risk analysis. However, it has been observed that certain simulated waste chemistries lead to significant change in open circuit potential (OCP) over time, and a steady-state value of OCP becomes the corrosion potential. A distinction is drawn between OCP and corrosion potential. At corrosion potential, rates of anodic and cathodic reactions balance each other, and the metal surface is in equilibrium with the surrounding electrolyte. OCP is defined when the metal surface is in process of establishing equilibrium with the surrounding electrolyte, and there is an imbalance between the rate of anodic and cathodic reactions. When the imbalance between anodic and cathodic reactions approaches zero, OCP becomes the corrosion potential of a metal surface in a given electrolyte. The change in OCP during CPP tests could lead to underassessment of the risk especially when corrosion potential is below the repassivation potential, and difference between the two is sufficiently low such that an upward drift in OCP would increase the risk of corrosion potential exceeding the repassivation potential, and thereby, increasing the risk of localized corrosion in form of pitting corrosion. Therefore, to quantify the risk of pitting corrosion due to OCP drift, laboratory experiments were conducted with a waste simulant composition with undetermined repassivation potential in CPP data.

Another key difference between laboratory testing using CPP and field conditions has been coupons surface condition used in the laboratory testing in comparison with the field condition of the tanks. CPP tests have been conducted using the bullet coupons with 600 grit polished surfaces,[2,3] whereas the tanks were constructed using the steel with mill scale plus corrosion products. It is recognized that during the construction process, large sheets of the carbon-steel metal were welded together, and other processes associated with tank construction could have disturbed the original mill-scale on the coupons. Considering this, a 600-grit polished coupon was utilized as one extreme of the surface condition whereas a coupon with mill-scale plus corrosion products is considered the other extreme. The surface condition of a newly constructed tank is expected to be somewhere between the two extremes. In addition, the tanks were put in service sometime after completion of construction. This would have provided the tank steel to get exposed to ambient conditions and develop additional layers or corrosion products before being placed in service. Considering several possibilities of the surface conditions, the objective of the study also included determining effect of surface condition on evolution of OCP. The objective also included establishing conservatism of the CPP tests results, i.e., the tests results sufficiently bound the conclusions derived from the test data. Details of the experiments and experimental data and results are described in the next two sections.

In addition to the experimental data collected for this work, literature information from prior studies is also documented. The literature information was sourced from several published and internal reports at Savannah River Site and the work conducted in support of the Hanford tank integrity program. Detail of the literature information is in the prior study section, followed by analysis and summary.

EXPERIMENTAL

Three corrosion cells were setup with three different electrodes, with each corrosion cell containing an electrode. Three coupons were prepared with each coupon acting as an electrode. The legacy carbon steel is fabricated from Association of American Railroads(1) Tank Car (AAR TC 128) steel since it approximates the chemistry and microstructure of the vintage steel from which the tanks were fabricated UNS K02401 (i.e., American Society for Testing and Materials (ASTM) (2) A515 Grade 60 carbon steel). Table 1 shows the chemical composition for the steel. All elemental compositions except for Mn and Si meet the ASTM specification. The three coupons differed with respect to each other in term of surface preparation. The first was a 600-grit polished bullet coupon, routinely used in the CPP tests. An image of the coupon is presented in Figure 1(a). The second was a cut out from a rail-road car steel piece with mill-scale and corrosion product on one face of the coupon. The second coupon was potted in epoxy with the exposed surface being the one with mill-scale plus corrosion products. An image of the

Table 1:Chemical Composition of AAR TC 128 Steel (wt.%)

	C	Mn	P	S	Si	Fe

---

(1) American Association of Railroads, 425 3rd Street SW, Washington, DC 20024

(2) ASTM International, 100 Barr Harbor Dr., West Conshohocken, PA 19428-2959

Specification	0.24 (max.)	0.9 (max.)	0.035 (max.)	0.04 (max.)	0.13 to 0.33	Balance
Measured	0.212	1.029	0.012	0.013	0.061	Balance

second coupon is presented in Figure 1(b). The third coupon was prepared in the same manner as the second coupon except that the part of the coupon surface was scuffed with 300 grit sand paper. This action was implemented to partially remove corrosion products and mill-scale on the coupon surface. Scuffing of the surface was to emulate potential changes to the surface during construction. An image of the third coupon is presented in Figure 1(c). The third coupon area which was scuffed with sand paper is highlighted by a red rectangle. The coupons are identified as following hereafter: (i) bullet (first), (ii) mill-scale (second), and (iii) partial mill-scale (third).

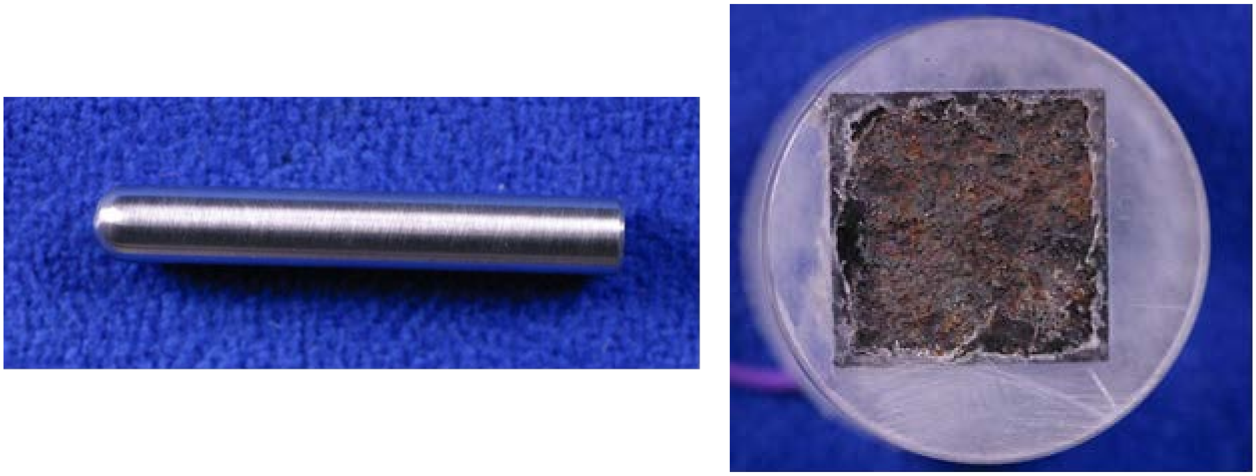

(a) 600 grit polished surface bullet coupon

(b) Coupon cut out of rail road car steel with mill-scale plus corrosion product on the exposed surface

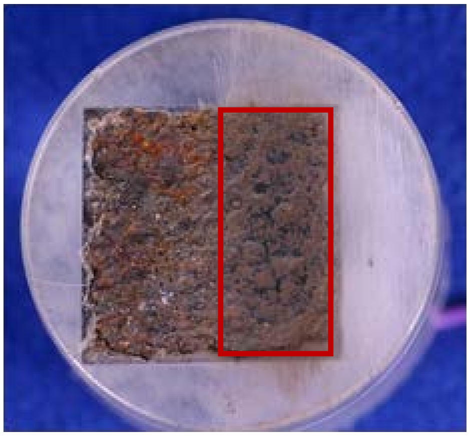

(c) Coupon cut out of rail road car steel with mill-scale plus corrosion product on the exposed surface. Part of the coupon surface, highlighted by red rectangle, was scuffed with 300 grit sand paper

Figure 1. Images of the three coupons used to study evolution of open circuit potential as a function of surface condition in AN-107 simulant

One of the key differences between the three coupons was immediately observed during resistance measurements. Two probes of a resistance meter were placed across thickness of the coupons, with one probe being on the exposed surface. Resistance of the bullet coupon was nearly independent of the probe positions and was less than 0.1 Ω in all measurements. Resistance of the mill-scale coupon varied with the position of the probe on the exposed surface, and resistance values ranged between 2.1 kΩ to 22.8 MΩ. Similarly, resistance of the partial mill-scale coupon also varied with the probe position and ranged between 60 to 580 Ω in areas where scuffing action was applied. The resistance values for the three coupons are listed in Table 2. The resistance data in Table 2 indicate that mill scale plus corrosion products provide a resistance barrier to charge flow, and even a slight scuffing of the surface changes resistance properties.

Table 2. Coupon Resistance Data	
Coupon	**Resistance (Ω) using a multimeter**
Bullet (no mill scale)	< 0.1 Ω
Mill-scale	20.7 MΩ, 2.1 kΩ, 22,6 MΩ, 21.5 MΩ, 22.8 MΩ
Partial mill-scale	60, 260, 580 Ω at the surface points were mill-scale was scuffed 4.4 and 10.5 kΩ at the mill-scale

The experiments were conducted using Hanford waste simulant as the electrolyte to study the evolution, i.e., drift of OCP. Chemical composition of the electrolyte is listed in Table 3.

Table 3. Chemical composition of the simulant used to study evolution of open circuit potential

Simulant source	Concentration (M)	Simulant source	Concentration (M)
Aluminum nitrate, 9-hydrate	0.1000	Disodium EDTA ($Na_2C_{10}H_{14}O_8.2H_2O$)	0.0540
Ferric nitrate, 9-hydrate	0.0310	HEDTA ($C_{10}H_{18}N_2O_7$)	0.0213
Calcium nitrate, 4-hydrate	0.0142	Nitrilotriacetic Acid	0.0085
Lead nitrate	0.0017	Iminodiacetic Acid	0.1265
Nickel nitrate, 6-hydrate	0.0094	Sodium gluconate	0.0284
Manganese dichloride	0.0139	Sodium hydroxide	2.1251
Potassium nitrate	0.0457	Sodium formate	0.4450
Sodium chloride	0.0222	Sodium acetate, 3-hydrate	0.0397
Sodium fluoride	0.0100	Sodium oxalate	0.0134
Sodium sulfate	0.0700	Sodium carbonate	1.4300
Sodium phosphate, 12-hydrate	0.0300	Sodium nitrate	2.5007
Glycolic acid	0.3080	Sodium nitrite	1.4000
Citric acid, 1-hydrate	0.1250		

All experiments were conducted at 35 °C, and atmospheric pressure. pH of the simulant was 13 at the start of the experiments.

EXPERIMENTAL DATA AND RESULTS

CPP data for the bullet coupon is presented in Figure 2. The data show the two duplicate runs. As seen in the figure, the CPP curves have mixed hysteresis, i.e., a clear delineation between pitting and no-pitting cannot be made. Both forward and return curves in the CPP data for the two runs overlap, indicating that CPP curves are inconclusive. Images of the bullet coupons immediately after the CPP tests are presented in Figure 3. As seen in Figures 3(a) and 3(c), coupons' surfaces developed coloration with tints of purple, green, and blue, but tiny micro-pits were observed at high magnification at the coupon surface.

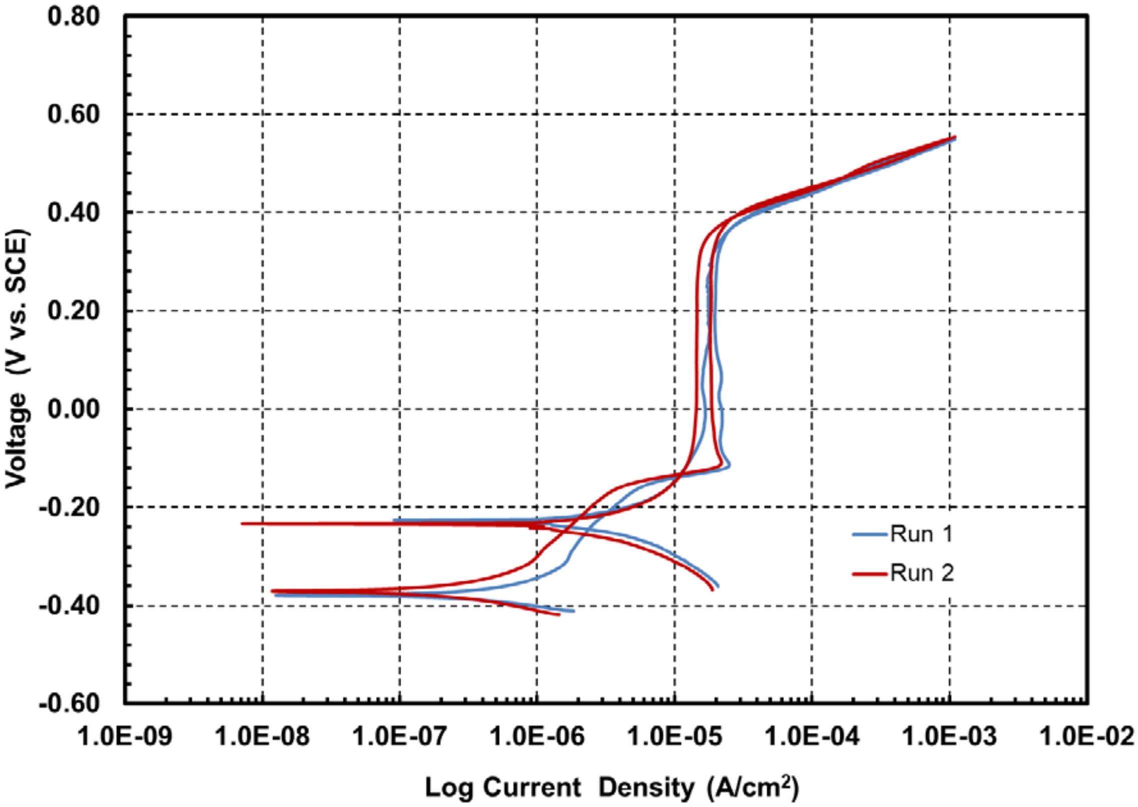

Figure 2. CPP data for the bullet coupon

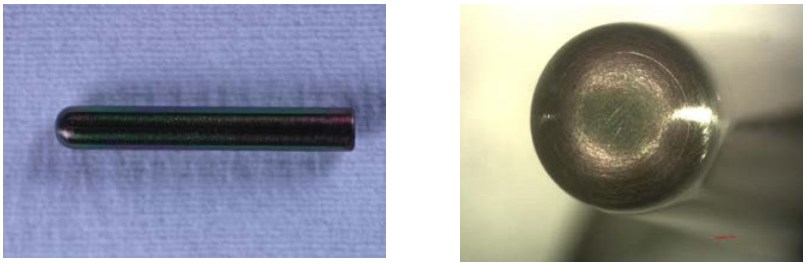

(a) Run 1 coupon side image **(b) Run 1 coupon nose image**

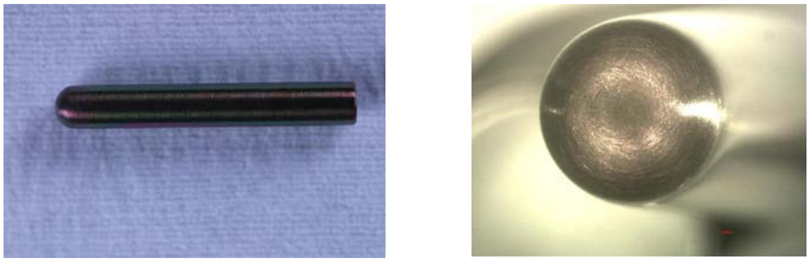

(c) Run 2 coupon side image **(d) Run 2 coupon side image**

Figure 3. Images of the bullet coupons immediately after CPP tests

The OCP data for the three coupons was collected for almost 70 days. The data for the bullet coupon are presented in Figure 4. As in the figure, the initial OCP is approximately -500 mV_{SCE}. The potential quickly rose to -320 mV and then stabilized at around -310 mV after several days.

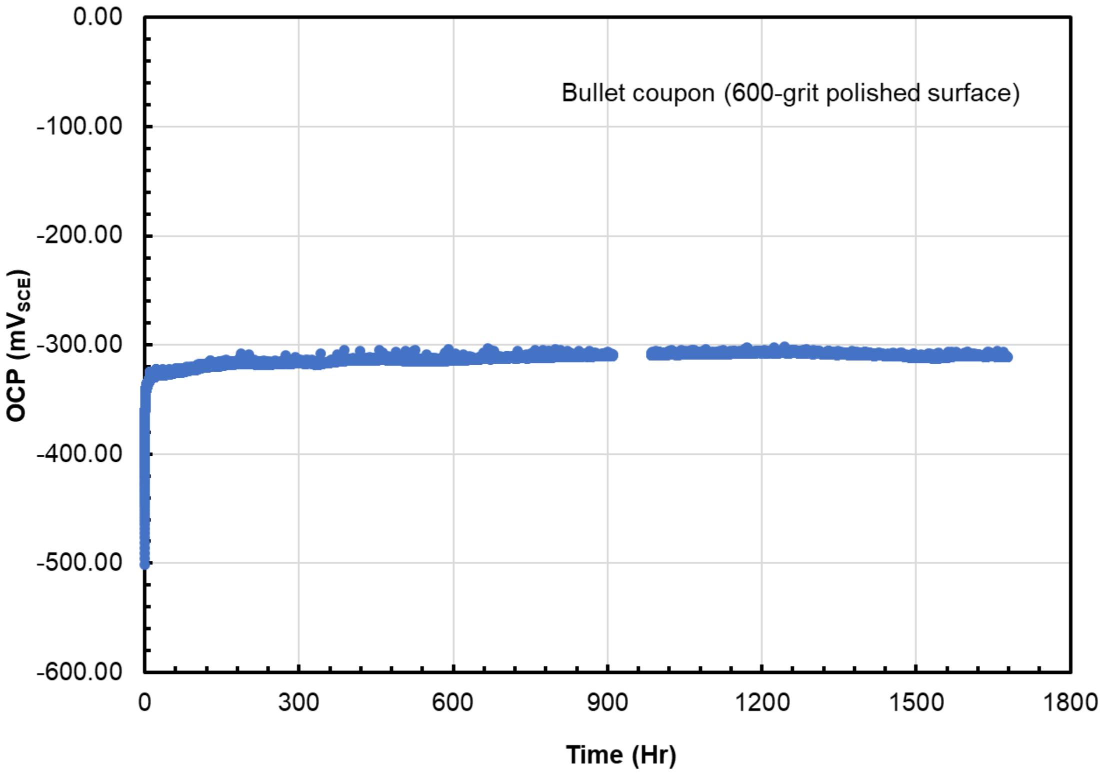

Figure 4. OCP data for the bullet coupon (600-grit polished surface)

OCP data for the mill-scale and partial mill-scale coupons are presented in Figures 5(a) and 5(b), respectively. In Figure 5(b) data for the two coupons have been superimposed for comparison. As seen in Figure 5(a) and 5(b), the OCP data for the coupons with pre-existing surface conditions such as mill-scale and corrosion products differed significantly compared to the bullet coupons with 600-grit polished surface. One of the key difference is the starting point for the OCP data. In Figure 4, the starting OCP value was more cathodic compared to the steady-state value. On other hand, terminal values of the OCPs are more cathodic compared to the initial values for mill- and partial mill-scale coupons. This indicate that the drift in OCP could either be cathodic or anodic, depending on the surface condition.

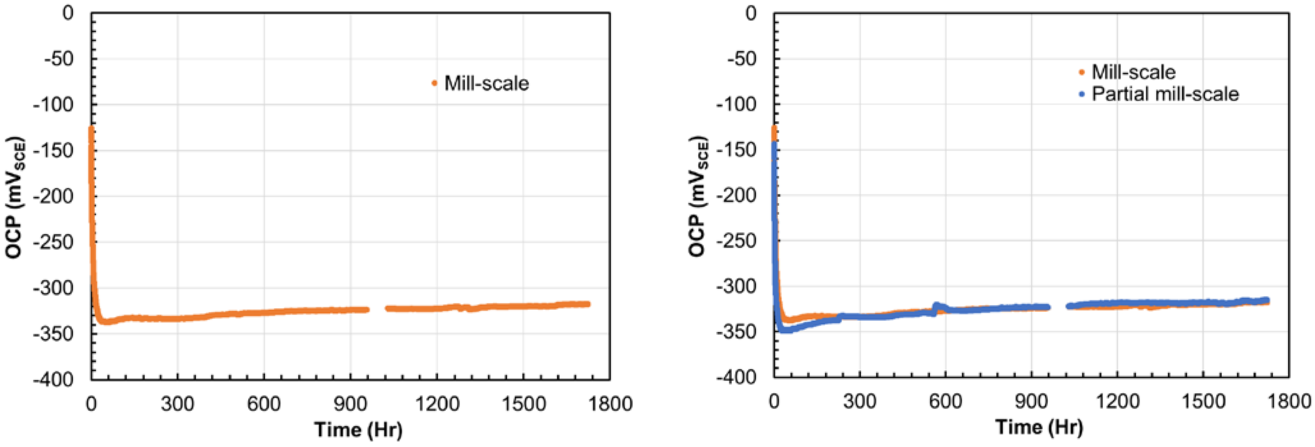

(a) OCP data for mill-scale coupon **(b) OCP data for mill- and partial mill-scale coupons**

Figure 5. OCP data for the mill- and partial mill-scale coupons

Magnitude of the drift as a function of time is highlighted. OCP data at several time instances are listed in Table 4, including terminal values. The OCP drift for the bullet coupon is 180 mV, with 139 mV of the drift occurring in the first 2 hours. The OCP drift for the mill-scale coupon is 192 mV, with only 87 mV drift in the first two hours compared to 139 out of 180 mV for the bullet coupon. Similarly, partial mill-scale coupon's OCP drifted by 172 mV, with 115 mV drift in the first two hours. Another point is that the terminal OCPs of the three coupons are within 10 mV of each other, indicating that terminal values are somewhat independent of the initial surface condition.

Table 4. Chemical composition of the simulant used to study evolution of open circuit potential

Time After Start (Hr)	Bullet Coupon OCP (mV_{SCE})	Mill-Scale Coupon OCP (mV_{SCE})	Partial Mill-Scale Coupon OCP (mV_{SCE})
0	-501.1	-125.5	-143.3
2	-340.6	-212.5	-258.6
24	-327.0	-329.2	-346.1
48	-323.9	-337.1	-348.2
72	-321.4	-336.0	-347.0
Terminal	-311.1 (at 1677 hr)	-317.7 (at 1722 hr)	-315.1 (at 1722 hr)

PRIOR STUDIES

Several prior studies have been reported with the same type of carbon-steel in the high-level waste simulant environments which are comparable to the simulant chemistry listed in Table 3. OCPs of U-bend coupons were recorded before measuring SCC susceptibility of the material.[4,5] The OCP data was collected at 50 °C, and is listed in Table 5. The OCP of all the samples became more noble or less negative over the course of the test, shifting between 80 to 207 mV more positive than the initial OCPs. The largest shifts occurred for coupons in solution with 0.1 M OH^- and 0.1 M NO_2^- and without the indents. These coupons also had OCP values that were more anodic than coupons in the 0.01 M OH^- plus 0.01 M NO_2^- and with indents. The data also indicate some effect of surface condition on the OCP drift. For example, the terminal values in 8.5 M NO_3^- plus 0.1 M OH^- plus 0.1 M NO_2^- for as-received and heat-treated samples differed by 54 mV, indicating some effect of surface condition on the corrosion potentials. It is noted that heat treatment not only causes difference in surface condition, but also can cause change in microstructure, both factors could affect OCP evolution.

Table 5. Open Circuit Potentials of U-bend Coupons

Solution Chemistry (M)			Surface Preparation*	OCP (mVSCE)	
$NaNO_3$	NaOH	$NaNO_2$		Initial	Final
5.5	0.01	0.01	AR, I	-332	-210
5.5	0.01	0.01	HT, I	-304	-216
8.5	0.01	0.01	AR, I	-309	-229
8.5	0.01	0.01	HT, I	-326	-221
8.5	0.1	0.1	AR, I	-305	-98
8.5	0.1	0.1	HT, I	-283	-152
8.5	0.01	0.01	AR	-312	-151
8.5	0.01	0.01	HT	-310	-128

* AR – as-received, HT – heat treated, I – indented

Another study on OCP evolution of A537 grade carbon steel in contact with the Hanford waste simulant was conducted.[6] The study included two different types of A537 steel: new A537 (A537 CL-1) and legacy/vintage A537 (A537 CL-2), with key difference being the surface condition between the new and vintage steel. The study test temperatures were 29 and 50 °C. The key difference between the current work and prior study was that the test solution and head space of the corrosion cells in the prior study were purged with Argon gas, thereby, removing any dissolved oxygen from the test solution. The OCP data were collected for 94 days. Initial and terminal OCP values are listed in Table 6.

Table 6. Open Circuit Potentials of new and vintage A537 steel in AN-107 simulant at 29 and 50 °C

Instance	OCP at 29 °C (mV_{SCE})		OCP at 50 °C (mV_{SCE})	
	New A537	Vintage A537	New A537	Vintage A537
Initial	-440 to -420	-440 to -420	-480 to -440	-440 to -420
Terminal	-440 to -420	-490 to -480	-450 to -440	-620

The data in Table 6 indicate that test temperature, surface condition, and deaeration play an important role in OCP evolution. The data also suggest that OCP evolution need not be anodic, and could be cathodic in de-aerated solutions. Data in Table 6 and the one in present study differ in one key area: Table 6 data was collected in solution which were de-aerated whereas the present study was conducted in the solution containing oxygen. Therefore, a one to one comparison is not made between the two studies, however, it is noted that evidence of cathodic evolution is present in Table 6 data.

Sridhar et al.[7] reported OCP data for railroad tank car carbon steel in several high-level waste simulants. The coupons used in the study included polished surfaces. The authors reported that OCPs increased considerably over time, sometimes as much as 400 mV. The authors attributed this evolution to enhancement of the passive film on the surface, in terms of film thickness, chemistry, or electronic properties. The final potential correlated reasonably well with the initial solution pH measured at the test temperatures, but did not correlate with any other parameters associated with chemistry of the test solution. The terminal OCP values in this work are consistent with data reported in Sridhar et al.[7]

SUMMARY

OCPs of railroad tank car (AAR TC 128) steel rail-road car carbon steel were measured in a Hanford waste simulant. Three coupons were fabricated whose surface condition differed with each other. OCP of the coupon with polished surface evolved in the anodic direction with respect to the initial value, whereas OCPs of the coupons with mill-scale plus corrosion products evolved in cathodic direction with respect to the initial values. Slight scuffing of the coupon with mill-scale plus corrosion products did not alter the OCP evolution direction, i.e., final OCP of the coupon was cathodic with respect to the initial value. The terminal OCPs of the three coupons were within 10 mV of each other, indicating that final OCPs were independent of the initial surface condition. This result is also consistent with the published literature where final OCPs correlated only with solutions' initial pH and temperature. The OCP evolution data also showed that most of the OCP change in the polished coupon occurred in first couple of hours. Since CPP tests are started two hours after setting up the experiments using a polished coupon, the wait time of two hours is deemed reasonably sufficient.

REFERENCES

---

1. ASTM International. ASTM G61 - 86(reapproved 2018), "Standard Test Method for Conducting Cyclic Potentiodynamic Polarization Measurements for Localized Corrosion Susceptibility of Iron-, Nickel-, or Cobalt-Based Alloys." West Conshohocken, Pennsylvania: ASTM International. 2018.

2. R. E. Fuentes, B. J. Wiersma, K. D. Boomer and A. J. Feero, "Inhibition of Pitting Corrosion in Simulated Liquid Radioactive Waste", CORROSION/2017, Paper No. 9689, NACE International, Houston, TX, 2017.

3. R. E. Fuentes, B. J. Wiersma, K. D. Boomer and A. J. Kim, "Pitting Corrosion Inhibition of Carbon Steel in Simulated Liquid Radioactive Waste at Elevated Hydroxide Concentrations", CORROSION/2018, Paper No. 51318-11456, NACE International, Houston, TX, 2018.

4. K.M. Counts, B.J. Wiersma, J.I. Mickalonis, "Determination of Corrosion Inhibitor Criteria For Type III/IIIA Tanks During Salt Dissolution Operations – Interim Report," Savannah River National Laboratory, WSRC-STI-2007-00552, Aiken, SC, 2007.

5. B.L. Garcia-Diaz, J.I. Mickalonis, B.J. Wiersma, "Determination of Corrosion Inhibitor Criteria For Type III/IIIA Tanks During Salt Dissolution Operations – Summary Document," Savannah River National Laboratory, SRNL-STI-2009-00600, REVISION 0, Aiken, SC, 2009.

6. H. Cong and S. Brossia, "FY2011 DNV DST Corrosion and Stress Corrosion Cracking Testing Report," Det Norske Veritas (U.S.A.) Inc., RPP-XXX-#####, Rev. A, 2011.

7. N. Sridhar, J.A. Beavers, B. Rollins, S. Chawla, K. Evans, and X. Li, "Stress Corrosion Cracking and Localized Corrosion of Carbon Steel in Nitrate Solutions." Corrosion, Vol. 27, No. 7, pp. 927-942, 2016.